Electronic Supplementary Material (ESI) for Soft Matter.

Supporting Information: Unsynchronous conformational transitions induced by the asymmetric adsorption-response of an active diblock copolymer in an inert brush

Shuanhu Qi,[†] Shuli Zhao,[‡] and Zengju Lian*,[‡]

†*School of Chemistry, Beihang University, Beijing 100191, China*

‡*School of Physical Science and Technology, Ningbo University, Ningbo 315211, China*

E-mail: lianzengju@nbu.edu.cn

Analytical theory for active diblock copolymer switches

Here we discuss the transition behavors for the systems corresponding to Scenario I, i.e. $N_c < N_b$, and II, i.e. $N_c > N_b$ and $N_B < N_b$ as defined in the main text. This starts from the construction of Landau type of free energy.

Here we present the results of the transition properties of the diblock copolymer chain for the two-state transitions, which are the cases of $N_B < N_b$ (meanwhile $N_c > N_b$, the scenario II) and $N_B > N_b$, $\alpha > \alpha_c$ (the scenario III). We discard the case for $N_c < N_b$ (scenario I), where only wide continuous phase transitions are observed. The SCF results are also compared with the analytical theory, and in all reasonably well match is obtained.

I. $N_c < N_b$**.** In this case, $N_A < N_b$ and $N_B < N_b$. The free energy expressed as a

function of n can be written as a step function

$$F(n)=\begin{cases} V_0N_c-\mu_AN_A-\mu_B(N_B-n)=F_{ads}+\mu_Bn, & 0\le n<N_B \\ V_0N_c-\mu_A(N_c-n)=F_{ads}+[\mu_B-\mu_A]N_B+\mu_An, & N_B\le n\le N_c \end{cases} \tag{S.1}$$

If μ_A and μ_B are bigger than zero, the function $F(n)$ obtains its global minimum at $n=0$, which specifies the adsorbed state, and increases monotonically with respect to n, i.e., no other stable state could appear. And if $\mu_A=\mu_B=0$, the curve of $F(n)$ becomes flat and independent of n, then the free energy for the adsorbed state at $n=0$ is equal to the extended state at $n=N_c$, which thus defines the transition point. Since the copolymer chain is shorter than the brush chains, the brush potential imposed on the copolymer can be viewed as a constant, which makes it similar to the case of a copolymer chain grafted on a brush-free surface. Therefore, the conformation transition is a continuous phase transition with wide transition width (data not shown), and the transition point is generally called the critical point. In the following we would not discuss further for such continuous phase transitions as they are not interested for the design of high performance switch sensors. It should be noted that because of the impenetrable boundary conditions, the SCF theory shifts the critical point to a finite value of adsorption strength, i.e. $\varepsilon_c>0$.

II. $N_c>N_b$ **and** $N_B<N_b$**.** To attain $N_c>N_b$, there are several ways by setting N_A and N_B properly, however, our study would demonstrate that the structure of the free energy $F(n)$ depends only on the length of the B block for the case of $N_c>N_b$. The phase behaviors can be partitioned into two scenarios according to the length of N_B relative to N_b, i.e. the scenario of $N_B<N_b$ and the scenario $N_B>N_b$. Here, we focus on the case of $N_B<N_b$, and leaving the discussion for $N_B>N_b$ later. If $N_B<N_b$, we can write the free

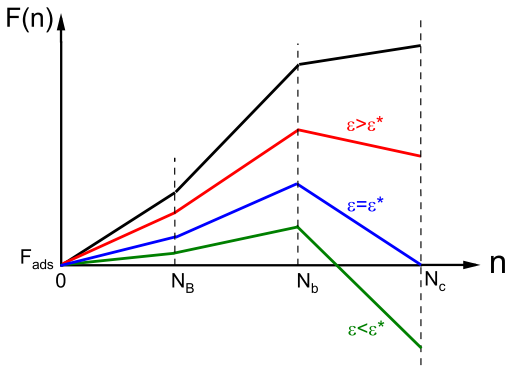

Figure S1: Sketch of the Landau free energy F as a function of the desorbed number of monomers n at different adsorption strength. Here, we take $N_{\rm c} > N_{\rm b}$ and $N_{\rm B} < N_{\rm b}$. The transition between the stable adsorbed state with $n = 0$ and the extended (exposed) state with $n = N_{\rm c}$ can be identified. The two-phase coexistence at the transition point $\varepsilon = \varepsilon^*$ signifies the first-order nature of the phase transition.

energy $F(n)$ as

$$F(n)=\begin{cases} V_0 N_{\rm c} - \mu_{\rm A} N_{\rm A} - \mu_{\rm B}(N_{\rm B} - n) = F_{\rm ads} + \mu_{\rm B} n, & 0 \le n < N_{\rm B} \\ V_0 N_{\rm c} - \mu_{\rm A}(N_{\rm c} - n) = F_{\rm ads} + [\mu_{\rm B} - \mu_{\rm A}] N_{\rm B} + \mu_{\rm A} n, & N_{\rm B} \le n < N_{\rm b} \\ V_0(N_{\rm c} + N_{\rm b} - n) - \mu_{\rm A}(N_{\rm c} - n) & \\ \quad = F_{\rm ads} + V_0 N_{\rm b} + [\mu_{\rm B} - \mu_{\rm A}] N_{\rm B} + [\mu_{\rm A} - V_0] n, & N_{\rm b} \le n \le N_{\rm c} \end{cases} \tag{S.2}$$

The profiles of $F(n)$ for different adsorption strength are sketched in Fig.S1, and two different stable conformational states, i.e. the adsorbed state, corresponding to $n = 0$ where all monomers are confined at the adsorption layer, and the extended state for $n = N_{\rm c}$, where the copolymer chain shows a stem-crown conformation, are clearly identified. According to Eq.S.2, $F(n)$ increases monotonically when $n < N_{\rm b}$ as the chemical potentials $\mu_{\rm A}$ and $\mu_{\rm B}$ are positive, after crossing $n = N_{\rm b}$, the tendency of $F(n)$ can be different depending on the sign of the slope $\mu_{\rm A} - V_0$. If the adsorption is weak $\mu_{\rm A} - V_0 \ll 0$, $F(n)$ decreases quickly and reaches a value at $n = N_{\rm c}$ that is smaller than $F_{\rm ads}$, i.e., $F(0) > F(N_{\rm c})$. This implies that at the weak adsorption, the extended state is the thermodynamically stable state (that is the equilibrium state). With the increase of adsorption strength and thus $\mu_{\rm A}$, the slope of

$F(n)$ with $n > N_\mathrm{b}$ changes positive, and $F(N_\mathrm{c})$ becomes larger. At some proper adsorption, one can get two minimums with equal value, i.e. $F(0) = F(N_\mathrm{c})$ showing the coexistence of the adsorbed and extended state, and we define such a state as the transition state. If the adsorption strength grows further, the free energy at $F(N_\mathrm{c})$ becomes even larger and finally $F(0)$ turns to be the global minimum suggesting that the adsorbed state becomes the thermodynamically stable one.

We define the adsorption that leads to the phase coexistence as the transition point ε^*, and the phase coexistence condition $F(0) = F(N_\mathrm{c})$ determines the transition point $\mu_\mathrm{A}(\varepsilon^*)N_\mathrm{A} + \mu_\mathrm{B}(\alpha\varepsilon^*)N_\mathrm{B} = V_0\Delta$, by using $\mu_\mathrm{i} \sim \varepsilon_\mathrm{i}$, one gets

$$\varepsilon^* = \frac{V_0\Delta}{N_\mathrm{A} + \alpha N_\mathrm{B}} \tag{S.3}$$

where $\Delta \equiv N_\mathrm{c} - N_\mathrm{b}$. When $\alpha = 0$, the B block monomers are inactive to the adsorption, we have the transition point $\varepsilon^* \sim V_0\Delta/N_\mathrm{A}$, and on the other limit when $\alpha = 1$, the transition point scales with respect to the total length of the diblock copolymer being $\varepsilon^* \sim V_0\Delta/N_\mathrm{c}$. These results agree with the predictions obtained in ref. S2. The transition barrier U_barrier is given by the free energy difference between the energy maximum at $n = N_\mathrm{b}$ and the energy minimum at $n = N_\mathrm{c}$ (or $n = 0$) at the transition point, i.e. $U_\mathrm{barrier} = [F(N_\mathrm{b}) - F(N_\mathrm{c})]_{\varepsilon=\varepsilon^*}$, resulting in

$$U_\mathrm{barrier} = \big[(\alpha - 1)N_\mathrm{B} + N_\mathrm{b}\big]\frac{V_0\Delta}{N_\mathrm{A} + \alpha N_\mathrm{B}} \tag{S.4}$$

For $\alpha = 0$, we have $U_\mathrm{barrier} \sim (N_\mathrm{b} - N_\mathrm{B})V_0\Delta/N_\mathrm{c}$, which matches the result obtained in ref. S1; and for $\alpha = 1$ with $\Delta \ll N_\mathrm{b}$, one gets $U_\mathrm{barrier} \sim V_0\Delta$, which is the situation that has been discussed in ref. S2.

To characterize the transition sharpness, we define the so called transition width as the change of adsorption parameter $\delta\varepsilon$, during which a reliable switching from the extended state with the average number of contacts (that is the average number of monomers confined in the adsorption layer) $\langle m\rangle = 0$ to the adsorbed state with $\langle m\rangle = N_\mathrm{c}$ is produced (here $\langle\cdots\rangle$

denotes the ensemble average). Therefore, $\delta\varepsilon$ can be extracted from the profile $\langle m\rangle$ with respect to the adsorption strength ε, and this is done as follows. First, one calculates the partition function of the copolymer system using $\mu_{\rm i} \sim \varepsilon_{\rm i}$ with ${\rm i} = {\rm A}, {\rm B}$

$$\begin{aligned} Z &= \sum_{n=0}^{N_{\rm c}} e^{-F(n)} = \frac{e^{\varepsilon_{\rm B}(N_{\rm B}+1)}-1}{e^{\varepsilon_{\rm B}}-1} e^{\varepsilon_{\rm A}N_{\rm A}-V_0N_{\rm c}} \\ &+ \frac{e^{\varepsilon_{\rm A}N_{\rm b}+V_0N_{\rm c}} - e^{\varepsilon_{\rm A}N_{\rm c}+V_0N_{\rm b}}}{e^{V_0}-e^{\varepsilon_{\rm A}}} e^{-V_0(N_{\rm c}+N_{\rm b}-1)-\varepsilon_{\rm A}N_{\rm b}} \\ &- \frac{e^{\varepsilon_{\rm A}N_{\rm B}} - e^{\varepsilon_{\rm A}N_{\rm b}}}{e^{\varepsilon_{\rm A}}-1} e^{\varepsilon_{\rm A}(N_{\rm A}-N_{\rm b})-V_0N_{\rm c}} \end{aligned} \tag{S.5}$$

Then the average number of contact monomer including A and B monomers is computed through

$$\langle m\rangle = \left[\frac{\partial \ln Z}{\partial \varepsilon_{\rm A}} + \frac{\partial \ln Z}{\partial \varepsilon_{\rm B}}\right]_{\varepsilon_{\rm A}=\varepsilon,\varepsilon_{\rm B}=\alpha\varepsilon} \tag{S.6}$$

According the definition, the transition width can be evaluated as the contact number difference between the states with $\varepsilon = \infty$ and $\varepsilon = 0$ divided by the absolute value of the slope of $\langle m\rangle$ at the transition point

$$\delta\varepsilon = \frac{\langle m\rangle_{\varepsilon=\infty} - \langle m\rangle_{\varepsilon=0}}{\left.\frac{\partial\langle m\rangle}{\partial\varepsilon}\right|_{\varepsilon=\varepsilon^*}} \tag{S.7}$$

The calculation of $\langle m\rangle$ and its derivative are complex. Suppose that we keep only the first order terms regarding the chain lengths and neglecting higher order terms such as that proportional to $N_{\rm b}^{-2}$, $N_{\rm B}^{-2}$, $N_{\rm A}^{-2}$, $(N_{\rm B}N_{\rm b})^{-1}$ and so on, we get an approximate expression for the transition width

$$\delta\varepsilon \simeq \frac{1}{N_{\rm A}+\alpha N_{\rm B}} \exp\left[\frac{\alpha V_0\Delta}{N_{\rm A}+\alpha N_{\rm B}}\right] \tag{S.8}$$

If the B block monomers are inert ($\alpha = 0$), we can obtain $\delta\varepsilon \sim N_{\rm A}^{-1}$, and on the other hand, if the B block monomers are identical to the A monomers ($\alpha = 1$), we would get $\delta\varepsilon \sim N_{\rm c}^{-1}$.

SCF thory and method

To test the theoretical predictions, we perform mean field SCF calculations.[S3,S4] In this method, polymer chains are assumed flexible and characterized by the continuous Gaussian model. Since the coupling of the single copolymer chain and the brush conformation, and thus the density and the potential are vanishingly small, we would treat the copolymer chain as an isolated chain immersed in a fixed potential including the contributions from substrate adsorption and brush repulsion. By doing so we can save a lot of computational time. The phase behaviors and transition properties of the active diblock copolymer are mainly extracted from the propagator $q^\dagger(z,s)$, which is the probability of finding the s-th monomer at position z. Under the mean-field description, the propagator $q^\dagger$ satisfies the following modified diffusion equation (MDE)[S3]

$$\frac{\partial q^\dagger(z,s)}{\partial z} = \frac{a^2}{6}\frac{\partial^2}{\partial z^2}q^\dagger(z,s) - \big(U_{\rm ads}^{\rm (i)} + V\big)q^\dagger(z,s) \tag{S.9}$$

with the Dirichlet boundary condition at $z = 0$ representing the impenetrability of the substrate and at $z = L_{\rm z}$ for another boundary, and $L_{\rm z}$ is chosen large enough that the free end of the copolymer chain is not able to reach there. The initial condition is set $q^\dagger(z, s = 0) = \delta(z - z_0)$, where z_0 denotes the position of the grafting point, and is set smaller than the Kuhn length a to approximate the location of the substrate $z = 0$ for numerical convenience. The adsorption potential $U_{\rm ads}$ is a stepwise function depending on the contour variable s, and $U_{\rm ads}^{\rm (i)}(z) = U_{\rm ads}^{\rm (A)}(z)$ for $0 \le s < N_{\rm A}$, and $U_{\rm ads}^{\rm (i)}(z) = U_{\rm ads}^{\rm (B)}(z)$ for $N_{\rm A} \le s \le N_{\rm c}$. The brush potential is obtained by solving the following SCF equations[S2]

$$\begin{aligned} V &= v_{\rm ex}\rho \\ \rho &= \frac{\sigma}{Q_{\rm b}}\int_0^{N_{\rm b}} ds q_{\rm b}^\dagger(z,s) q_{\rm b}(z, N_{\rm b} - s) \end{aligned} \tag{S.10}$$

where v_{ex} is the excluded volume parameter as defined before, and we choose $v_{\mathrm{ex}} = 1$. ρ is the brush monomer density. The single chain propagators for brush chains $q_{\mathrm{b}}^{\dagger}$ and q_{b} satisfy the same form of the MDE but with a different potential

$$\frac{\partial q(z,s)}{\partial s} = \frac{a^2}{6}\frac{\partial^2 q(z,s)}{\partial z^2} - V(z)q(z,s) \tag{S.11}$$

where $q \equiv q_{\mathrm{b}}^{\dagger}, q_{\mathrm{b}}$. Dirichlet boundaries are applied along the z direction, and the initial condition for $q_{\mathrm{b}}^{\dagger}$ is chosen $q_{\mathrm{b}}^{\dagger}(z, s=0) = \delta(z - z_0)$ representing the grafting of the one chain end, and for $q_{\mathrm{b}}(z,s)$, it is $q_{\mathrm{b}}(z, s=0) = 1$ showing the uniform distribution of the free end in the system. The single chain partition function Q_{b} relates to the propagator $q_{\mathrm{b}}^{\dagger}$ through $Q_{\mathrm{b}} = \int dz q_{\mathrm{b}}^{\dagger}(z, N_{\mathrm{b}})$.

In terms of the propagator of the copolymer chain $q^{\dagger}$, one can obtain the distribution of the A/B block joint point $P_{\mathrm{j}}(z) \equiv q^{\dagger}(z, N_{\mathrm{A}})$ and of the free end $P_{\mathrm{e}}(z) \equiv q^{\dagger}(z, N_{\mathrm{c}})$. The average height of the joint point Z_{j} and the free end Z_{e} can be calculated as

$$Z_{\mathrm{j}} = \frac{\int dz z q^{\dagger}(z, N_{\mathrm{A}})}{\int dz q^{\dagger}(z, N_{\mathrm{A}})} \tag{S.12}$$

and

$$Z_{\mathrm{e}} = \frac{\int dz z q^{\dagger}(z, N_{\mathrm{c}})}{\int dz q^{\dagger}(z, N_{\mathrm{c}})} \tag{S.13}$$

The transition point and transition barrier are extracted from P_{j} and P_{e} for the transition regarding the conformation of A block and the whole copolymer chain, respectively. To make this more clearly, let consider the phase transition of the whole copolymer chain as an example. At the transition point, the distribution function P_{e} would exhibit a bimodal structure, where the two maximums representing the two coexisting state states are equal in magnitude. Then we define the particular adsorption strength ε^* which leads to such bimodal distribution as the transition point. In addition, from P_{e}, one obtains the Landau free energy $U_{\mathrm{L}} = -\ln P_{\mathrm{e}}(z)$. The transition barrier is defined as the energy barrier that needs

to overcome when passing from one stable state to the other stable state at the transition point ε^*. The transition width is evaluated through the profile of $Z_{\rm e}$ with respect to ε, and this is done as follows. First, one finds the slope of $Z_{\rm e}$ at the transition point ε^*, and then calculates the transition width according to

$$\delta\varepsilon = \frac{Z_{\rm e}\big|_{\varepsilon=0} - Z_{\rm e}\big|_{\varepsilon=\infty}}{-\frac{\partial Z_{\rm e}}{\partial \varepsilon}\Big|_{\varepsilon=\varepsilon^*}} \tag{S.14}$$

Similar methods can be adopted to analyze the transition properties of the A block monomers through $P_{\rm j}$ and $Z_{\rm j}$,

It may be noted that in the theoretical treatment, we use the average number of contact monomers $\langle m \rangle$ or the torn-off monomers n as the variable parameter to define phases and quantify the transition properties. Here, in the SCF method, we choose the height of the joint monomer or the free end monomer for convenience. These two methods, although lead to quantitatively different results, should predict the same phase behaviors, for example, they would give the same scaling relations concerning the transition point, transition barrier and transition width with respect to the system parameters, as they represent the intrinsic and general physics laws of the transition properties. This also rationalizes the qualitative comparison between the results obtained from theoretical treatment and SCF calculations.

SCF results for the transition properties

Conformational state and transition types of the second Scenario

Then we consider the second scenario, i.e., $N_{\rm c} > N_{\rm b}$ and $N_{\rm B} < N_{\rm b}$. In this case, the analytical theory predicts that two stable states, the extended state and the adsorbed state, would be recognized during the phase transitions of the copolymer chain by varying the adsorption strength, and such transition can occur independent of the adsorption ratio. To verify the theoretical predictions, we plot in Fig.S2 the average height of the joint point and the free

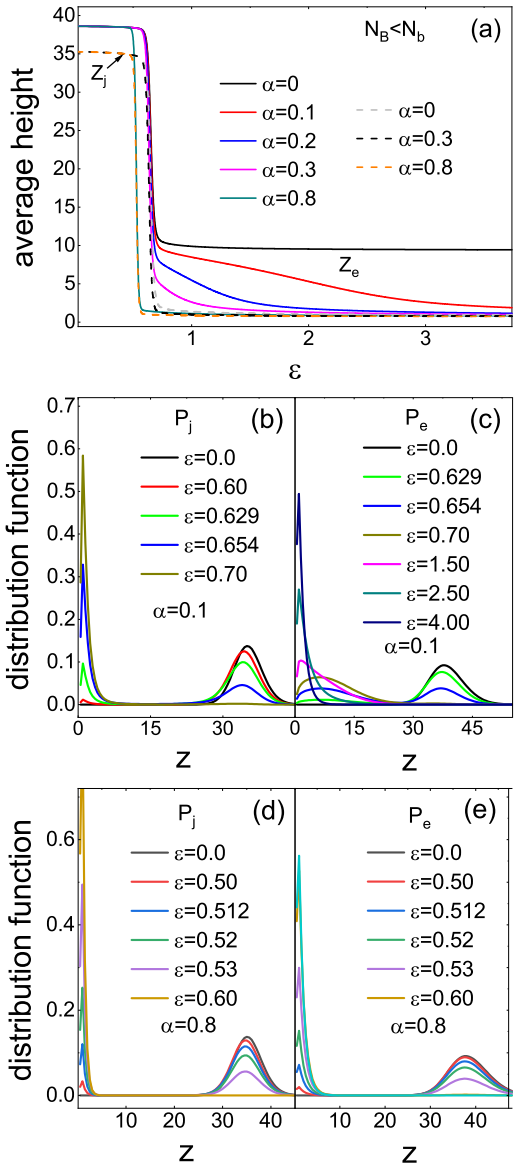

Figure S2: Average height of the A/B block joint point Z_{j} (dashed lines) and the free end monomer Z_{e} (solid lines) for different adsorption ratio α (a), the distribution of A/B block joint monomer P_{j} for $\alpha = 0.1$ (b) and $\alpha = 0.8$ (d), and the distribution of the free end P_{e} for $\alpha = 0.1$ (c) and $\alpha = 0.8$ (e). Other parameters are set as follows: $N_{\mathrm{A}} = 110$, $N_{\mathrm{B}} = 80$, $N_{\mathrm{b}} = 100$, so $N_{\mathrm{c}} > N_{\mathrm{b}}$ and $N_{\mathrm{B}} < N_{\mathrm{b}}$ are satisfied. The grafting density of the brush is chosen $\sigma = 0.1$. The results are obtained by SCF calculations.

end as well as their distributions obtained by SCF calculations.

In Fig.S2a, the solid lines present the average height of the free end Z_{e} as a function of adsorption strength ε for several different α from small $\alpha = 0$ to large $\alpha = 0.8$. These curves show that when the adsorption is weak, Z_{e} is almost flat, and it then decreases dramatically within a narrow interval of ε before approaching to a final constant value again. The two plateau regions observed in the curve Z_{e} signify a two-state transition between the extended state with a stem-crown conformation at $\varepsilon = 0$ confirmed by the fact that $Z_e(\varepsilon = 0) \approx 38.5$ being larger than the height of the brush for $N_{\mathrm{b}} = 100$ and $\sigma = 0.1$, and the adsorbed state at sufficiently large ε where Z_{e} is close to zero. The two-state nature of the transition holds varying α from 0 to 1.

The transition is sharp as the absolute value of the slope of Z_{e} in the transition region is large especially when α is large or exactly zero. In fact, when α is small, e.g., close to zero, the adsorption imposing on B block monomers is smaller than that on A block monomers, thus the B monomers attach to the substrate only when ε is large enough, and this leads to the long smooth declining tail in the curve of Z_{e}. The tail becomes shorter as α increases and finally vanishes as $\alpha \to 1$ which induce sharp transition of the copolymer. In contrast, if $\alpha = 0$, B monomers would never aggregate into the adsorption layer and the residual Z_{e} in the high adsorption region comes only from the B block. Meanwhile, the residual Z_{e} keeps fixed inducing a second platform in Z_{e} curve as the adsorption strength beyond the transition point which results in a second stable state. Consequently, the long declining tail is not observed in this situation which results in sharp phase transitions of the A block chain. To show the transition sharpness of the A block chain during the conformation transition, we also plot in Fig.S2a the average height of the joint monomer Z_{j} using dashed lines, and sharp transitions are clearly confirmed. For a certain α, Z_{j} and Z_{e} get overlapped in the transition region meaning that their transition points are almost the same. We would note that the state that only A monomers being adsorbed in the adsorption layer as $\alpha > 0$ is not a thermodynamically stable state, the investigation of the transition width regarding

the conformation transitions of the A block is still valuable, for example, for the design of sensitive switch sensors exploiting the conformation transition of the A block chain.

The conformation phases and their transitions can also be identified through the distribution function of the joint monomer $P_{\rm j}$ and that of the end monomer $P_{\rm e}$. For illustration, we plot in Fig.S2b, S2c, S2d, and S2e $P_{\rm j}$ and $P_{\rm e}$ with a small adsorption ratio $\alpha = 0.1$ and a large one $\alpha = 0.8$ as denoted in these figures. The enhanced distribution peak near $z = 0$ with a small ε and at $z \simeq 35$ with a large ε in Fig.S2c and Fig.S2e represents the adsorbed state and extended state, respectively. The bimodal structure of P_e illustrates clearly the phase coexistence and an energy barrier (corresponding to the minimum between the two peaks in $P_{\rm e}$) between the two stable states, and these imply the first-order nature of the phase transitions. The transition point extracted from $P_{\rm e}$ when the two maximums have the same magnitude gives $\varepsilon^* \simeq 0.512$ for $\alpha = 0.8$, which is smaller than $\varepsilon^* \simeq 0.654$ for $\alpha = 0.1$, and such results agree with the prediction from Fig.S2a that large α shifts the transition point ε^* to a low value.

The distribution $P_{\rm j}(z)$ shares similar features with $P_{\rm e}(z)$, for example, unimodal and bimodal structures are observed at proper ε, however, these structures just specify some conformation states of the copolymer chain showing no information about their stability, and the stability could be detected by other means, for example, through the free energy $F(n)$. In Fig.S2b, one can see that the conformation transition of the A block monomers happens about $\varepsilon^* \simeq 0.629$, which is close to $\varepsilon^* \simeq 0.654$ extracted from the conformation change of the whole chain. Similar situation holds for $\alpha = 0.8$, where $P_{\rm j}$ and $P_{\rm e}$ give the same transition point, i.e. $\varepsilon \simeq 0.512$ (see Fig.S2d and Fig.S2e). This means that the A block and B block switch conformations under almost the same adsorption strength, which is consistent to the observed two-state transition in the system.

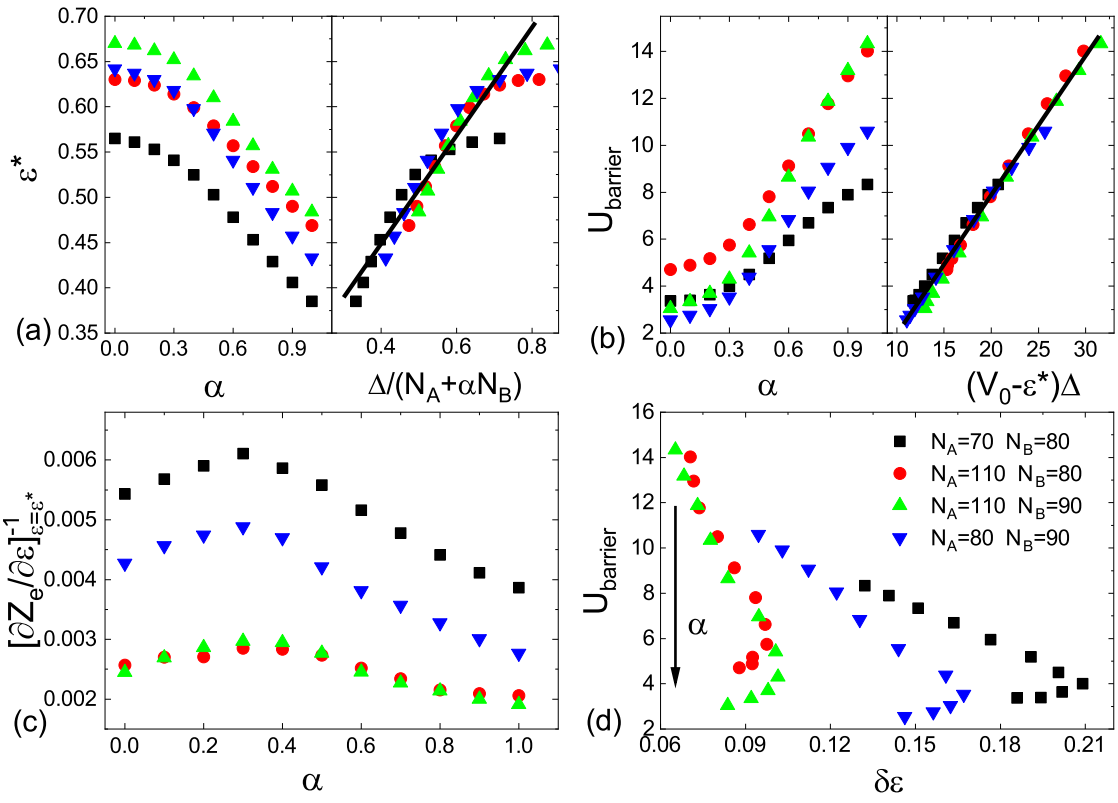

Figure S3: Transition point ε^* (a) and transition barrier $U_{\rm barrier}$ (b) for the transitions between the extended state and the adsorbed state for $N_{\rm B} < N_{\rm b}$ and $N_{\rm c} > N_{\rm b}$ extracted from $P_{\rm e}(z)$. The scaling plots for ε^* and $U_{\rm barrier}$ are also shown. The inverse of the absolute value of the slope $Z_{\rm e}$ v.s. ε at the transition point ε^* defined as $l^{-1} \equiv |\partial Z_{\rm e}/\partial\varepsilon|^{-1}_{\varepsilon=\varepsilon^*}$ (c), and the transition barrier as a function of the transition width $\delta\varepsilon$ with $\delta\varepsilon \equiv [Z_{\rm j}(\varepsilon = 0) - Z_{\rm j}(\varepsilon = \infty)]l^{-1}$. The brush chain length is chosen $N_{\rm b} = 100$ and the grafting density $\sigma = 0.1$. All the data are obtained by SCF calculations. Solid lines are obtained by data fitting to guide the eyes.

Two-state transitions for $N_{\mathrm{B}} < N_{\mathrm{b}}$

Let us first present the transition properties for the case $N_{\mathrm{B}} < N_{\mathrm{b}}$. As being shown in the main text, under such parameter, there are only two stable phases observed during the phase transitions, one is the extended state (fully desorbed state), and the other is the adsorbed state. It is thus convenient to extract the transition point and transition barrier from $P_{\mathrm{e}}(z)$. Fig.S3a shows the transition point as a function of α for different block lengths N_{A} and N_{B} as denoted. As can be seen the transition point ε^* is a monotonically decreasing function of α, which is expected, as the increase of α would effectively increases the adsorption strength imposed on B-block monomers thus decreases the critical energy to meet the requirement of producing the phase transition. If $\alpha \to 0$, the analytical theory gives $\varepsilon^* \propto 1 - \frac{N_{\mathrm{b}} - N_{\mathrm{B}}}{N_{\mathrm{A}}}$ (see Eq.S.3), i.e., ε^* increases with N_{A} or N_{B}, when the other one is fixed, and such relation is definitely verified in Fig.S3a. On the other hand, if $\alpha = 1$, the analytical theory predicts $\varepsilon^* \propto 1 - N_{\mathrm{b}}/N_{\mathrm{c}}$ (see Eq.S.3) indicating that ε^* increases monotonically with N_{c}, which also agrees with the SCF results. In the right panel of Fig.S3a, we replot the same data shown in the left panel with the scaling coordinates as suggested by the analytical theory (see Eq.S.3). All data points with different A/B block lengths collapse reasonably well onto a single master curve, implying the consistence between the predictions from the analytical theory and the SCF calculations.

Fig.S3b left panel displays the transition barrier at the transition point as a function of α. Obviously, for given N_{B} in the figure which are close to N_{b}, the transition barrier grows monotonically with respect to α which matches the theoretical prediction shown in Eq.S.4 $U_{\mathrm{barrier}} \simeq \Delta V_0/(\frac{N_{\mathrm{A}}}{\alpha N_{\mathrm{B}}} + 1)$ under the approximation $N_{\mathrm{b}} - N_{\mathrm{B}} \simeq 0$. At the limits of $\alpha = 0$ and $\alpha = 1$, U_{barrier} shows different dependence on the chain block lengths, for example, at $\alpha = 0$ for any fixed N_{A}, U_{barrier} sometime has a negative relation with N_{B} (in fact, the transition barrier at $\alpha = 0$ changes non-monotonically with N_{B}, and it is similar to the situation of $\alpha = 0.1$ which we will discuss later), while at $\alpha = 1$, U_{barrier} becomes an increasing function of N_{c}. These results match the theoretical prediction shown in Eq.S.4,

which gives $U_{\rm barrier} \propto (N_{\rm b} - N_{\rm B}) - (N_{\rm B} - N_{\rm b})^2/N_{\rm A}$ for $\alpha = 0$ and $U_{\rm barrier} \propto 1 - N_{\rm b}/N_{\rm c}$ for $\alpha = 1$. Low energy barrier only shows up when α is small for given $N_{\rm B}$ and $N_{\rm A}$ in Fig.S3, for example $U_{\rm barrier}$ can be smaller than $3k_{\rm B}T$ when $\alpha < 0.3$. The small energy barrier is mainly controlled by the B block length $N_{\rm B}$, and it could be even smaller when $N_{\rm B} \to N_{\rm b}$. Thus, practically useful design of switch sensors may be restricted to the small α region and the length $N_{\rm B}$ not very far from that of $N_{\rm b}$. In Fig.S3b right panel we replot the transition barrier with respect to the scaled coordinate as suggested by the theoretical prediction (see Eq.S.4), and the SCF data are quite close to collapsing onto a single straight line illustrating the nice matching between the analytical theory and the SCF results.

To measure the sharpness of the transition, we calculate the inverse of the slope of $Z_{\rm e}$ v.s. ε at the transition point ε^*, i.e. $l^{-1} \equiv |\frac{\partial Z_{\rm e}}{\partial \varepsilon}|^{-1}_{\varepsilon=\varepsilon^*}$, and plot l^{-1} as a function of α in Fig.S3c. In fact, the transition width during this transition is not clearly defined especially when α is small, because of the long slowing varying tail showing in $Z_{\rm e}$. It shows that l^{-1} is not a monotonic function of α, and exhibiting a maximum at some intermediate value $\alpha \simeq 0.3$, which may be related to the long-decreasing tail in $Z_{\rm e}$ (see Fig. 4a in the main text). At $\alpha = 0$, the free end of B block will never reside in the adsorbed layer, and the transition width can be defined through $\delta\varepsilon = [Z_{\rm e}(\varepsilon = 0) - Z_{\rm e}(\varepsilon = \infty)]/l \simeq N_{\rm A} l^{-1}$, and the analytical theory predicts that $\delta\varepsilon \simeq N_{\rm A}^{-1}$ indicating $l^{-1} \simeq N_{\rm A}^{-2}$. This can be testified qualitatively by the SCF results shown in Fig.S3c, where at $\alpha = 0$ for both $N_{\rm B} = 80$ and $N_{\rm B} = 90$, the transition width is smaller if $N_{\rm A}$ is larger. On the other limit of $\alpha = 1$, the conformations of A block and B block change synchronously and the copolymer behaviors as a homopolymer, thus the transition width can be well defined by $\delta\varepsilon \simeq N_{\rm c} l^{-1}$, and the analytical theory predicts $\delta\varepsilon \simeq N_{\rm c}^{-1}$ implying a negative relation between l^{-1} and $N_{\rm c}$, which matches the SCF data shown in Fig.S3c for $\alpha = 1$. If we multiply l^{-1} by $N_{\rm A}$ at small α region and by $N_{\rm c}$ at the region α approaching 1, we would see that the transition width $\delta\varepsilon$ roughly increase with α, implying that sharp transitions happen when α is small.

To see the relation between $U_{\rm barrier}$ and $\delta\varepsilon$. we combine Fig.S3b and Fig.S3c together in

Fig.S3d by setting U_{barrier} as the vertical axis and $\delta\varepsilon = [Z_{\text{j}}(\varepsilon = 0) - Z_{\text{j}}(\varepsilon = \infty)]l^{-1}$ as the horizontal axis, and thus $\delta\varepsilon$ is meaningful only in the small α region. In Fig.S3d it can be seen that in the small α region, a low free energy barrier, e.g. smaller than $3k_{\text{B}}T$ is obtained when N_{B} approaches N_{b}, and sharp transitions, e.g. around 0.1 is attained when N_{A} is larger than N_{b}, for example $N_{\text{A}} = 110$. This means that the transition barrier and the transition width are decoupled and controlled by different parameters. This is probably the reason that U_{barrier} and $\delta\varepsilon$ are positively correlated when α is small contrary to their negative relation in first order transitions happened in macroscopic systems. From the practical point of view, a positive correlation has advantages for the design of high performance switch sensors as this allows the improvement of material sensitivity and response speed simultaneously.

To see the influence of chain block lengths N_{A} and N_{B} on the transition properties as well as considering a practically interesting situation, we choose $\alpha = 0.1$, and plot ε^*, U_{barrier}, and $\delta\varepsilon$ respectively in Fig.S4a, S4b, S4c as a function of N_{B} with different N_{A}. Here $\delta\varepsilon$ is defined as $\delta\varepsilon = [Z_j(\varepsilon = 0) - Z_{\text{j}}(\varepsilon = \infty)]l^{-1}$.

In Fig.S4a left panel, one can see that ε^* is a monotonically increasing function of N_{B}, and the dependence of ε^* on N_{A} at fixed N_{B} agrees with the analytical prediction of ε^* in the small α limit (see Eq.S.3). The U_{barrier} becomes a quadratic curve with respect to N_{B} with the location of its maximum moving to small values of N_{B} when N_{A} is increased, and this can be testified by the analytical expression of U_{barrier} (see Eq.S.4). The well collapse of different points shown in Fig.S4a and Fig.S4b right panels onto two single master curves, which satisfy the scaling relation expressed by Eq.S.3 and Eq.S.4, respectively, confirms also good matching between the theory and the SCF method. In Fig.S4b, it clearly shows that U_{barrier} drops sharply when N_{B} approaches N_{b}, i.e. small U_{barrier} can be found when N_{B} is close to N_{b}, and there U_{barrier} has just very weak dependence on N_{A}, for example, the points for different N_{A} at $N_{\text{B}} = 90$ are quit close to each other. This illustrates again the N_{B} is more relevant in reaching a low transition barrier. On the other hand, as shown in Fig.S4c, $\delta\varepsilon$ has weak dependence on N_{B}, while strongly relates to N_{A}, and the larger N_{A}, the smaller

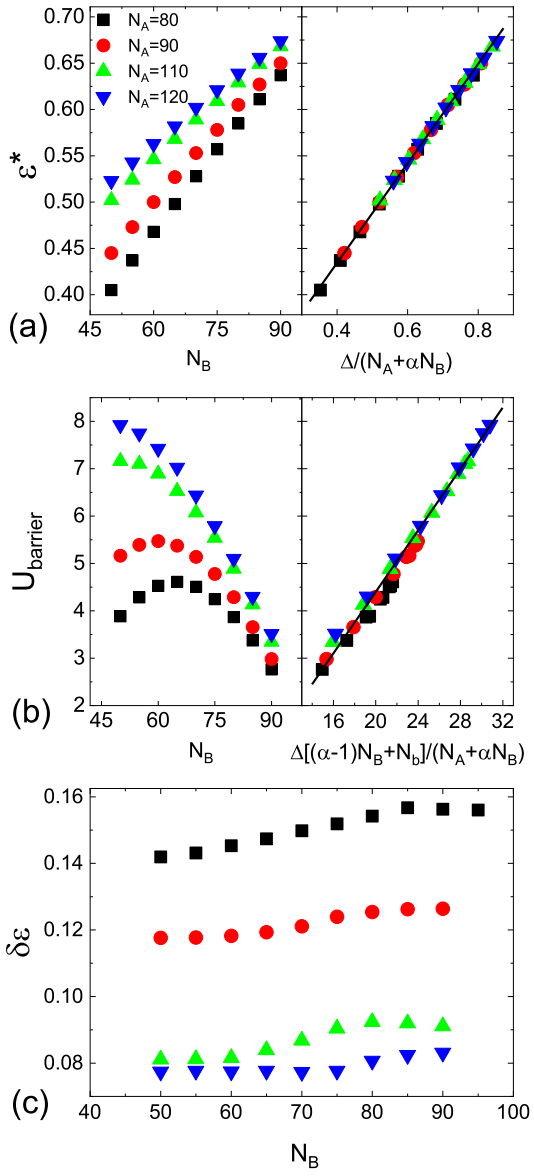

Figure S4: Transition point ε^* (a) and transition barrier $U_{\rm barrier}$ (b) for the transitions between the extended state and the adsorbed state extracted from $P_{\rm e}(z)$. The scaling plots for ε^* and $U_{\rm barrier}$ are also shown on the right panels. The transition width is defined as $\delta\varepsilon = [Z_j(\varepsilon = 0) - Z_{\rm j}(\varepsilon = \infty)]l^{-1}$ (c). The adsorption ratio is set small $\alpha = 0.1$, the brush chain length is chosen $N_{\rm b} = 100$, and the grafting density $\sigma = 0.1$. All the data are obtained by SCF calculations. Solid lines are obtained by data fitting to guide the eyes.

$\delta\varepsilon$. These results further demonstrate that sharp transitions with low energy barrier can be realized when α is small, $N_{\rm B}$ is close to $N_{\rm b}$, and $N_{\rm A}$ being larger than $N_{\rm b}$.

Two-state transitions for $N_{\rm B} > N_{\rm b}$ and $\alpha > \alpha_{\rm c}$

Then we consider the transition properties of a diblock copolymer with $N_{\rm B} > N_{\rm b}$ corresponding to the scenario III. Analytical theory and SCF calculations have demonstrated that the phase behaviors are qualitatively different depending on the parameter α, i.e., if $\alpha < \alpha_{\rm c}$ three-state transitions happen, and if $\alpha > \alpha_{\rm c}$ two-state transitions are observed. The critical value of $\alpha_{\rm c}$ can be estimated according to the theoretical expression Eq.5 in main text, for example, if $N_{\rm b} = 100$, $N_{\rm B} = 110$, one has $\alpha_{\rm c} \simeq 0.091$, and for $N_{\rm b} = 100$, $N_{\rm B} = 120$, one gets $\alpha_{\rm c} \simeq 0.167$. SCF calculations lead to a larger $\alpha_{\rm c}$, which is already seen in the phase diagram (see Fig.6a in the main text). In the following, we only focus on the two-state transition, that is the transition of the whole chain between the extended state and the adsorbed state for $\alpha > \alpha_{\rm c}$.

Fig.S5a presents the dependence of ε^* on the scaling coordinate as suggested by the analytical theory (see Eq.14 in the main text). Still, it can be seen that the transition point is a decreasing function of α. Different points obtained for different $N_{\rm A}$ and $N_{\rm B}$ fall reasonably well onto single straight lines, although these lines can not get perfectly overlapped. The exact reason for the deviation between theory and SCF calculations is not clear, but the neglection of logarithm corrections in the theory may be partly responsible for this.

Fig.S5b left panel displays that the transition barrier $U_{\rm barrier}$ grows fast with respect to α when $\alpha > \alpha_{\rm c}$. Such result agrees with the theoretical prediction shown in Eq.15 in the main text. According to this equation $U_{\rm barrier}$ obtained for $\alpha > \alpha_{\rm c}$ should be proportional to $\alpha\varepsilon^*$, and this is confirmed by the scaling plot of $U_{\rm barrier}$ in the right panel of Fig.S5b, where data points fall into a straight lines. These results tell that to achieve a low barrier transition, one should consider to take a small α.

Fig.S5c shows the transition width $\delta\varepsilon$ as a function of α with $\alpha > \alpha_{\rm c}$. It can be seen

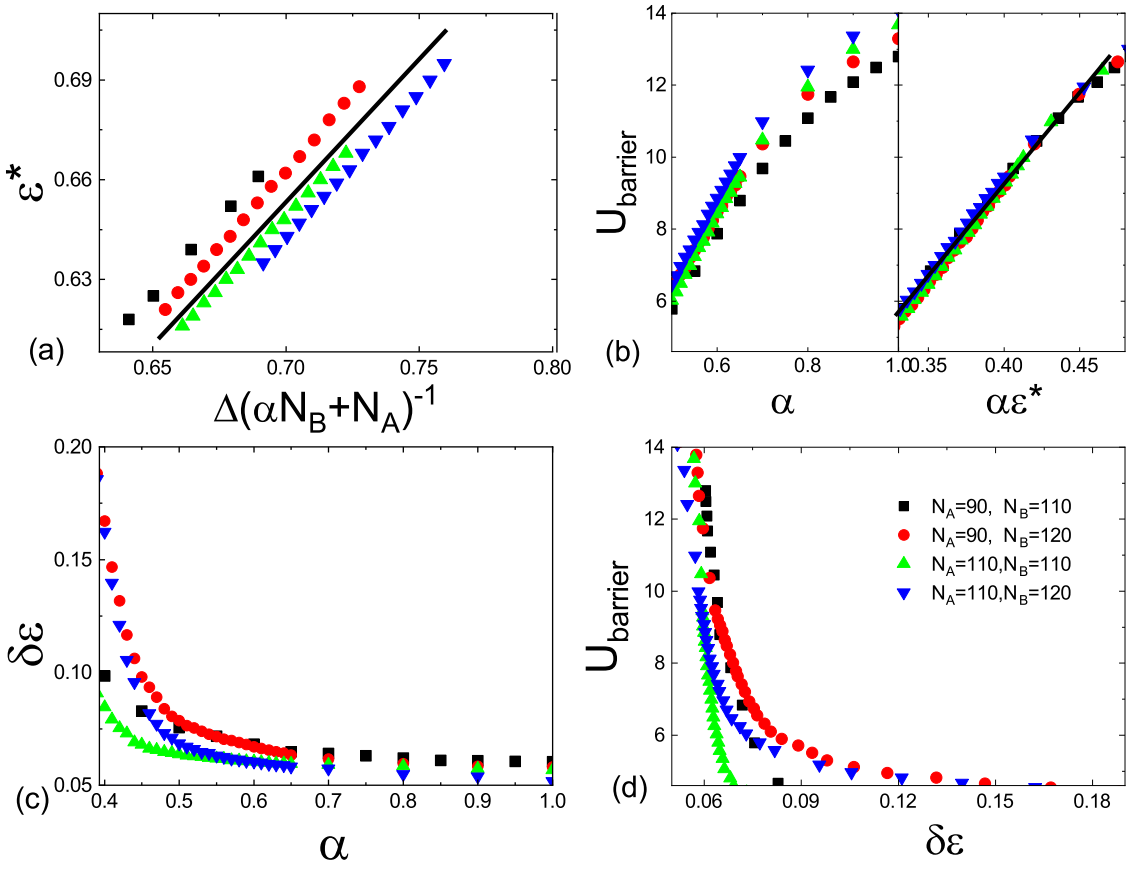

Figure S5: Transition point ε^* (a), transition barrier $U_{\rm barrier}$ (b), and transition width $\delta\varepsilon$ plotted according to different coordinates as denoted in the case of $N_{\rm B} > N_{\rm b}$ with $\alpha = 0.5 > \alpha_{\rm c}$. The transition barrier is plotted as a function of the transition width $\delta\varepsilon$ in (d). The critical value $\alpha_{\rm c}$ are parameter dependent, for $N_{\rm B} = 110$, $\alpha_{\rm c}$ is estimated around 0.37, and $\alpha_{\rm c} \simeq 0.40$ for $N_{\rm B} = 120$. Other parameters are set $N_{\rm b} = 100$, $\sigma = 0.1$. All the data are obtained by SCF calculations. Solid lines are obtained by data fitting to guide the eyes.

that $\delta\varepsilon$ decreases quickly and keeps a low constant almost independent of α when passes the critical point α_c. The final transition width is about 0.07 corresponding to a sharp transition. The irrelevance of $\delta\varepsilon$ with respect to α observed as $\alpha > \alpha_c$ is the result of the competition of the exponential term and its prefactor of the transition width shown in Eq.16 in the main text. The form has a positive relation with α while the later has a negative relation with α. Combining Fig.S5b with Fig.S5c, we get that U_{barrier} and $\delta\varepsilon$ are negatively correlated. Fortunately, the transition width decreases sharply and saturates to a low value when α is not far away from the critical value α_c, where the transition barrier is not quite enhanced (see Fig.S5d). So, one can get a fast and low-barrier two-state switch by choosing α a litter larger than the critical value.

To illustrate clearly the influence of N_A and N_B on the transition properties, we plot in Fig.S6 the transition point, transition barrier, and transition width respectively as a function of N_B for several chosen N_A ranging from short $N_A < N_b$ and long $N_A > N_b$ blocks. We consider the transition of the whole copolymer chain corresponding to the case $\alpha > \alpha_c$ (see Fig.S5), and so we use $\alpha = 0.5 > \alpha_c$.

Fig.S6a and Fig.S6b left panels show that ε^* and U_{barrier} share similar behaviors with respect to N_B. For example, they have weak dependence on N_A when N_B is relatively small (close to the length of brush chains N_b), and become irrelevant of N_A when N_B is large. In fact, according to the analytical theory, ε^* and U_{barrier} assume a similar expression for fixed α, that is $\varepsilon^*,\ U_{\text{barrier}} \propto \frac{\Delta}{N_A+\alpha N_B}$. If α is large, for example $\alpha > \alpha_c$, we could take $\alpha \simeq 1$, and in this case, one has $\varepsilon,\ U_{\text{barrier}} \simeq 1 - \frac{N_b}{N_A+N_B}$, which is an increasing function of N_A or N_B given the other one fixed. The dependence of ε and U_{barrier} on N_A definitely becomes weaker when N_B increases, which qualitatively agrees with the SCF results. In the right panels of Fig.S6a and Fig.S6b, we replot ε^* and U_{barrier} in terms of the scaling parameters suggested by the analytical results Eq.14 and Eq.15 in the main text, and data points do not exactly collapse into a single master curve showing quantitative deviation from the theory and SCF calculations.

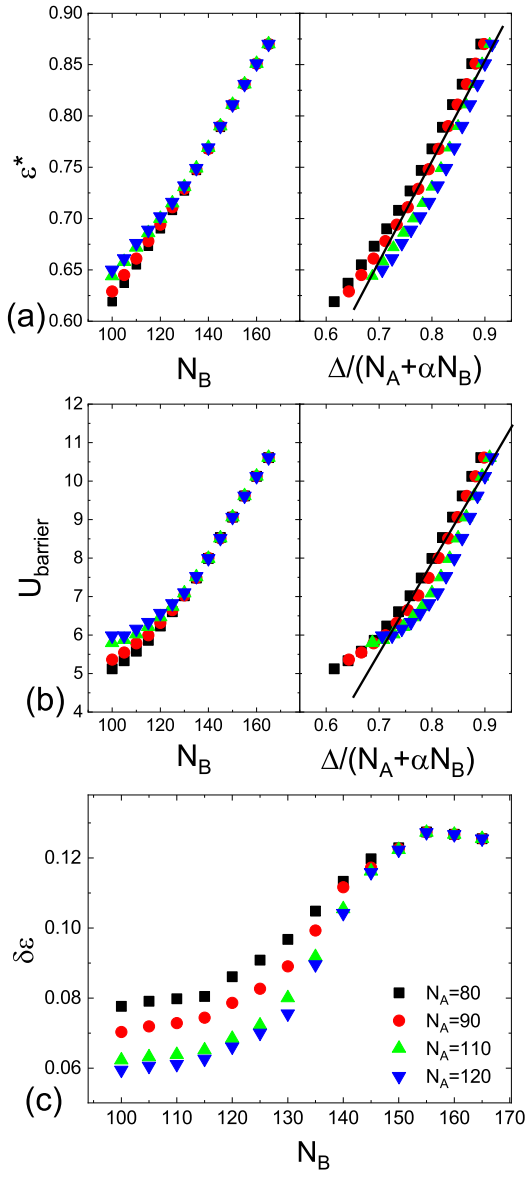

Figure S6: Transition point ε^* (a), transition barrier U_{barrier} (b) plotted as a function of N_{B} (left panels) and according to the scaled coordinates suggested by analytical theory (right panels) in the case of $N_{\text{B}} > N_{\text{b}}$. Transition width $\delta\varepsilon$ is plotted as a function of N_{B} (c), U_{barrier} expressed as a function of $\delta\varepsilon$. These transitions correspond to the transition of the copolymer chain between the extended state and adsorbed state at large α, i.e., $\alpha = 0.5 > \alpha_{\text{c}}$. The transition properties are extracted from Z_{e} and P_{e}. Other parameters are set $N_{\text{b}} = 100$, $\sigma = 0.1$. All the data are obtained by SCF calculations. Solid lines are obtained by data fitting to guide the eyes.

Fig.S6c plots $\delta\varepsilon$ as a function of $N_{\rm B}$. For a fixed $N_{\rm A}$, $\delta\varepsilon$ increases slowly a bit with $N_{\rm B}$ increasing at first and then decreases as $N_{\rm B}$ increases further. In the analysis prediction of Eq.16 in the main text, the transition width $\delta\varepsilon$ is in proportion to the product of two factors: one is $g_1 = (N_{\rm A} + \alpha N_{\rm B})^{-1}$ and the other is $g_2 = \exp\left[\alpha V_0(1 - \frac{N_{\rm b}}{N_{\rm A}+N_{\rm B}})\right]$. g_1 decreases with $N_{\rm B}$ while g_2 increases with $N_{\rm B}$. According SCF results, it indicates that g_2 dominates the transition width at small $N_{\rm B}$ while g_1 plays main role at large $N_{\rm B}$. Similarly, for a fixed $N_{\rm B}$, the change trend of $\delta\varepsilon$ with change of $N_{\rm A}$ is determined by the competition of g_1 and g_2 (g_1 decreases with $N_{\rm A}$ and g_2 increases with $N_{\rm A}$ for the parameters indicated in Fig.S6). The decreasing of $\delta\varepsilon$ with increasing of $N_{\rm A}$ at fixed $N_{\rm B}$ shows that g_1 dominates in $\delta\varepsilon$ for present parameters.

The positive correlation between $U_{\rm barrier}$ and $\delta\varepsilon$ indicates that sharp transitions are always accompanied by low transition barriers, which is favorable for the design of high performance switching materials. However, the absolute value of $U_{\rm barrier}$ is large under the present chosen parameters, for example, for $N_{\rm A} = 80$, $N_{\rm B} = 105$, $U_{\rm barrier} \simeq 5k_{\rm B}T$ although the transition is sharp about $\delta\varepsilon \simeq 0.08$. Considering also the previous results we get that to attain sharp and low-barrier transitions one need to take a small α.

Chain lengths dependence of the transition properties for $N_{\rm B} > N_{\rm b}$ and $\alpha < \alpha_{\rm c}$

The chain lengths of A block and B block are also important parameters of the system. Here, we focus on the influence of $N_{\rm A}$ and $N_{\rm B}$ on the transition properties of the B block. For such a purpose, we plot in Fig.S7 the transition point, transition barrier, and transition width respectively as a function of $N_{\rm B}$ for several chosen $N_{\rm A}$ ranging from short $N_{\rm A} < N_{\rm b}$ to long $N_{\rm A} > N_{\rm b}$ blocks. Here we choose $\alpha = 0.1$ which is smaller than $\alpha_{\rm c}$.

Fig. S7 shows that the transition point ε_2^*, transition barrier $U_{\rm barrier}$, and transition width $\delta\varepsilon_{\rm B}$ are all independent of the A block length $N_{\rm A}$, which is quite obvious, as A monomers always keep their adsorbed conformation and not at all involved when the B block experiences

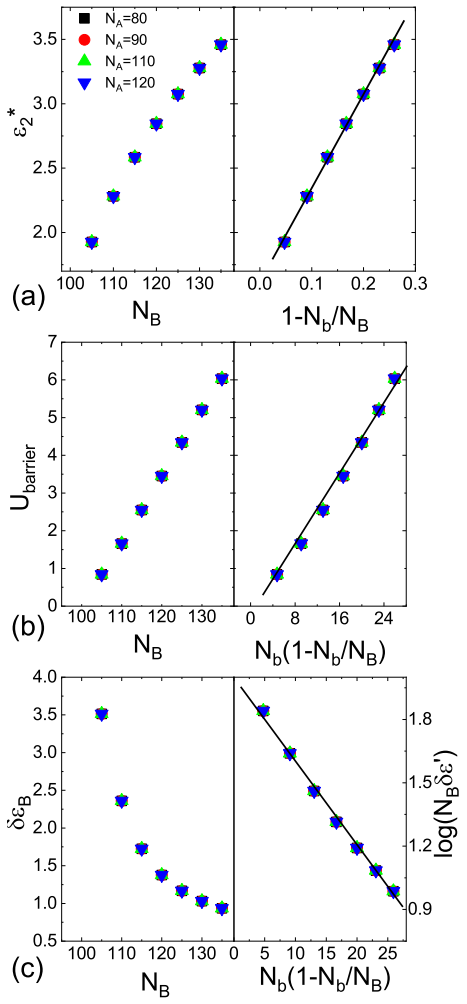

Figure S7: Transition point ε_2^* (a), transition barrier $U_{\rm barrier}$ (b), and transition width $\delta\varepsilon_{\rm B}$ (c) plotted as a function of $N_{\rm B}$ (left panels) and according to the scaled coordinates suggested by analytical theory (right panels). The transition considered is the transition of the B block between the extended state and the adsorbed state at small α, i.e., $\alpha = 0.1 \leq \alpha_{\rm c}$, that is the transition between the mixed state and the adsorbed state from the point view of the whole copolymer chain. These transition properties are extracted from $Z_{\rm e}$ and $P_{\rm e}$. Here $\delta\varepsilon' = 0.23(\delta\varepsilon_{\rm B} - 0.62)$. Other parameters are set $N_{\rm b} = 100$, $\sigma = 0.1$. All the data are obtained by SCF calculations. Solid lines are obtained by data fitting to guide the eyes.

the transition between the extended state and the adsorbed state. Fig.S7a left panel shows that ε_2^* is a monotonically increasing function of $N_{\rm B}$, which is expected, as longer $N_{\rm B}$ requires more energy to trigger the transition. Fig.S7b shows that $U_{\rm barrier}$ approaches zero, when the length of the B block $N_{\rm B}$ is close to the length of the brush chains $N_{\rm b}$, and it grows fast when $N_{\rm B}$ is much larger than $N_{\rm b}$. This tell us that to achieve a small energy barrier, one needs to take the length $N_{\rm B}$ not far from $N_{\rm b}$. On the other hand the transition width $\delta\varepsilon_{\rm B}$ decrease monotonically with respect to $N_{\rm B}$ as displayed in Fig.S7c. In the right panels of Fig.S7a, Fig.S7b, and Fig.S7c, we replot ε_2^*, $U_{\rm barrier}$ and $\delta\varepsilon_{\rm B}$ with respect to the scaled coordinate suggested by Eq.10, Eq.11, and Eq.13, respectively, and the obtained straight lines demonstrate good consistent between the analytical theory and SCF calculations. The negative correlation of $U_{\rm barrier}$ and $\delta\varepsilon_{\rm B}$ results that to get optimization of a switch, one has to carefully balance the transition width and transition barrier to obtain a sharp transition with low energy barrier.

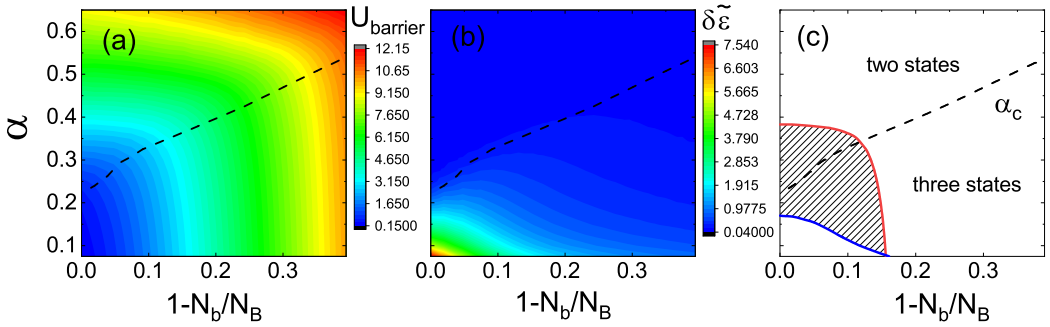

Figure S8: Contour plots of the transition barrier (a), transition width (b). Parameter space resulting in high performance transitions with sharp width ($\delta\tilde{\varepsilon} < 0.1$) and low barrier $U_{\rm barrier} < 3k_{\rm B}T$ is represented by the shallow region in (c). Other parameters are set $N_{\rm A} = 110$, $N_{\rm b} = 100$, and $\sigma = 0.1$. The dashed line gives the critical curve of $\alpha_{\rm c}$ extracted from the SCF results. In (c) the red line denotes $U_{\rm barrier} = 3k_{\rm B}T$, and on the left side of this line, the transition barrier is smaller than $3k_{\rm B}T$. The blue line denotes $\delta\tilde{\varepsilon} = 0.1$, and on the right side of this line, the transition width is larger than 0.1. These contour figures are plotted according to the data obtained by SCF calculations. Note that $\delta\tilde{\varepsilon} \equiv \delta\varepsilon_{\rm B}$ for $\alpha < \alpha_{\rm c}$ and $\delta\tilde{\varepsilon} \equiv \delta\varepsilon$ for $\alpha > \alpha_{\rm c}$.

To have a perceptual view of the transition barrier and transition width for the conformation transitions of the B block with $\alpha < \alpha_{\rm c}$ (meaning that the data for the B block transition

shown in the main text are included) and the transitions concerning the whole copolymer chain with $\alpha > \alpha_c$, and particularly finding out the parameter space where sharp transitions with low energy barrier can be accomplished, we scan the controlling parameters in a more wide space and perform contour plots for the transition barrier U_{barrier} and transition width $\delta\tilde{\varepsilon}$ ($\delta\tilde{\varepsilon} \equiv \delta\varepsilon_B$ for $\alpha < \alpha_c$ and $\delta\tilde{\varepsilon} \equiv \delta\varepsilon$ for $\alpha > \alpha_c$) in Fig.S8. Since N_A would not change the structure of the free energy and thus keeps the nature of the conformation transitions, we therefore choose an arbitrary length of the A block, i.e., $N_A = 110$, and it is expected that only quantitative difference may be observed if one set N_A to another value. Fig.S8a shows the dependence of U_{barrier} with respect to α and $1 - N_b/N_B$, and it can be seen that U_{barrier} increases roughly along the line $\alpha = 1 - N_b/N_B$, meaning that to obtain a low-barrier transition, one may choose small α and short N_B (i.e., approaching N_b). In contrast, the transition width $\delta\tilde{\varepsilon}$ decreases roughly along the line $\alpha = 1 - N_b/N_B$ for $\alpha < \alpha_c$, and thus sharp transitions appear when α and N_B are large for $\alpha < \alpha_c$. The negative correlation between U_{barrier} and $\delta\tilde{\varepsilon}$ implies that a compromise has to be made for the optimization of the transition performances. We define the low barrier as $U_{\text{barrier}} < 3$ and the sharp width if $\delta\tilde{\varepsilon} < 0.1$, then we find the parameter space leading to sharp transitions with low transition barrier in Fig.S8c represented by the shadow region. Roughly speaking, high performance transitions can be attained in both two-state and three-state transitions in the parameter space within a small region covering the line α_c when α is small, and N_B close to N_b.

References

(S1) S. Qi, L. I. Klushin, A. M. Skvortsov, and F. Schmid, *Macromolecules*, 2020, **53**, 5326-5336.

(S2) S. Qi, L. I. Klushin, A. M. Skvortsov, A. A. Polotsky, and F. Schmid, *Macromolecules*, 2015, **48**, 3775-3787.

(S3) G. Fredrickson, *The equilibrium theory of inhomogeneous polymers*, New York, Oxford University Press, 2006.

(S4) F. Schmid, *J. Phys.: Cond. Matter*, 1998, **10**, 8105-8138.